

Efficient GaN tunnel junctions using embedded GdN nanoislands

Sriram Krishnamoorthy,^{1,a)} Jing Yang², Pil Sung Park,¹ Roberto Myers^{2,1} and Siddharth Rajan^{1,2,b)}

¹Department of Electrical & Computer Engineering, The Ohio State University, Columbus, OH 43210

²Department of Material Science & Engineering, The Ohio State University, Columbus, OH 43210

Abstract: Highly efficient inter-band tunneling in GaN using epitaxial GdN nanoislands embedded in a degenerately doped PN junction is reported. PN tunnel junctions oriented in both the Ga-polar and N-polar orientation had low resistance, indicating weak polarity dependence. The GaN/GdN/GaN tunnel junction was used to replace the p-contact in a pn junction diode, and a low tunneling specific resistivity of $2.7 \times 10^{-3} \Omega\text{-cm}^2$ was measured. This is the lowest specific tunneling resistivity reported till date for GaN. The low tunneling resistance achieved using this approach could enable new designs for increased functionality and performance in wide band gap electronic and optoelectronic devices.

^{a),b)} Authors to whom correspondence should be addressed. Electronic mail: krishnamoorthy.13@buckeyemail.osu.edu; rajan@ece.osu.edu

Inter-band tunnel junctions (TJ) in a broad range of material systems such as Ge¹, III-As² and SiGe³ rely on degenerate doping of the PN junction to lower the tunneling barrier to increase tunneling current. Since depletion width (and, consequently, tunneling current density) depends on impurity concentration, the dopant solubility limits the maximum current drive obtainable in such tunnel junctions. Recent work on staggered gap materials has addressed this issue by using heterostructure line-ups to enhance tunneling between conduction and valence bands⁴.

In the wide band gap III-nitride system, use of tunnel junctions in applications such as LEDs⁵ and solar cells⁶ has been prevented by the larger band gap that leads to thicker depletion region, large energy barriers to tunneling and hence higher tunneling resistance than in lower gap semiconductors. Recently, the spontaneous and piezoelectric polarization^{7,8} in the III-nitride system using structures like GaN/AlN/GaN^{9,10}, GaN/InGaN/GaN^{11,12}, and AlGaIn/GaN¹³ were successfully used to overcome limitations imposed by the large energy band gap. Among these approaches, GaN/InGaN/GaN tunnel junctions were found to give the best performance due to large interface polarization charges and low band gap in the InGaN layer. In polarization-engineered tunnel junctions, the polarization-induced field acts in the same direction as the PN depletion field, thereby reducing the depletion width greatly (to a few nm).

While the polarization-based approach using InGaN leads to very low resistance¹⁴, the dependence on crystal orientation could present significant limitations in certain cases since the direction of polarization field while using InGaN as the barrier material is fixed for a given orientation. For instance, in order to incorporate a tunnel junction contact to p-type GaN for a p-down Ga-polar LED structure¹⁵ or a p-up N-polar c-plane LED structure¹⁶, the GaN/InGaN/GaN structure would not be effective since the polarization field in such cases would oppose the depletion field. In this work, we show that tunneling can be enhanced using mid-gap states that have weak dependence on the polarization, and therefore on the crystal polarity.

Mid-gap states have been used in the past to enhance tunneling in several ways, including low temperature (LT) MBE grown GaAs¹⁷, and epitaxial semi metallic ErAs^{18,19} and MnAs nanoparticles in

GaAs²⁰. Active devices such as solar cells²¹ were epitaxially grown above the tunnel junction to demonstrate the feasibility of utilizing such structures for high quality device applications. Mid-gap states enable design of interband tunnel structures that can overcome limitations imposed by the fundamental energy gap and dopant solubility, and could therefore be expected to enhance tunneling in large band gap semiconductors such as GaN.

In this work, we demonstrate the use of rare earth pnictide (GdN) nanoislands in a degenerately doped PN junction for enhanced tunneling, and the use of a tunnel junction in a device (PN junction diode), resulting in very low specific contact resistivity for any III nitride tunnel junction demonstrated till date. Among the rare earth nitrides, GdN, which has a cubic rock salt structure, is the most studied material and has been proposed for spintronic applications^{22,23}. Bandstructure calculations reveal that bulk GdN is an indirect semiconductor with an band gap of 0.7-0.85 eV²⁴. (111) oriented GdN has a 9.4% lattice mismatch with the basal plane of wurtzite GaN, and is therefore expected to grow in a Volmer Weber growth mode²⁵. Growth of GdN nanoislands has also been previously demonstrated with single crystalline GaN layer overgrown on the nanoislands²⁶, in contrast to polycrystalline GaN overgrown on planar (111) GdN²⁵.

To calculate the energy band diagram of a GaN/GdN/GaN heterojunction, we model GdN as a non-polar material with a narrow bandgap, and assume that the polarization discontinuity at the GaN/GdN interface leads to an interface charge density that is equal to the spontaneous polarization sheet charge of GaN. This is depicted in the charge diagram in Fig 1 (a) and (b), for the Ga-face and N-face oriented PN junctions, respectively. For p-GaN up structure, the field due to the spontaneous polarization sheet charge dipole $\sigma_{sp,GaN}$ is in the same direction as that of the depletion field in case of N- polar, where as the direction is opposite in the case of Ga – polar structure. The effect of doping in GaN on the band diagram is shown in Fig. 1 (c) and (d) for Ga polar and N polar case respectively, assuming equal conduction band offset and valence band offset and a dielectric permittivity²⁴ of 7. The depletion width is expected to be lower in the N-polar case than in the Ga-polar case, with the difference being less significant as the

doping density is increased. At the highest doping density shown ($N_D = N_A = 5 \times 10^{19} \text{ cm}^{-3}$), the depletion field exceeds the polarization field and the band diagram looks similar for both the orientations, and the depletion width is not significantly different in the two cases. Under forward bias, holes in the valence band of p-GaN and electrons in the conduction band of n-GaN tunnel into states in GdN and recombine. Since the forward bias current does not rely on direct band to band tunneling (from n-GaN to p-GaN), we do not expect band-crossing related negative differential resistance (as expected in a normal heterojunction Esaki diodes). In reverse bias, electrons in the valence band of p-GaN tunnel into conduction band of n-GaN via states in GdN.

GaN PN junctions with high doping density were grown along N face and Ga face orientations using a Veeco GEN930 Plasma Assisted Molecular Beam Epitaxy (PAMBE) with ultra-thin GdN layer inserted at the p^+ -GaN/ n^+ -GaN interface. The epitaxial stack is shown in Fig. 2 (a). GdN nanoislands were grown on n-doped GaN with a growth rate of 0.4 ML/min on a n-doped GaN/Sapphire template²⁷. GdN coverage was incomplete and deposition of 2.4 ML of GdN resulted in a partially coverage with 3 nm tall islands oriented along the [111] direction on wurtzite [0001] GaN. Details about island formation dynamics and transmission electron microscope images of the islands grown are described elsewhere²⁶. Single crystalline p-type GaN was grown on top of the GdN nanoislands, as observed by in-situ reflection high-energy electron diffraction. The structure was capped with heavily doped GaN to enable the formation of a low resistance ohmic contact. The epitaxial stack shown in Fig 2 (a) was also grown along the N-polar orientation on a free standing N-polar GaN template from Saint Gobain²⁷. The device was processed using contact lithography, with Ti(20nm)/Au(200nm) ohmic contact for the GaN:Si layer and Ni(20nm)/Au(200nm) ohmic contact on p^{++} GaN cap.

The electrical characteristics of the GaN/GdN/GaN TJ ($20 \mu\text{m} \times 20 \mu\text{m}$) on both polarities are shown in Fig. 2(b). At a reverse bias of 1 V, the Ga-polar GaN/GdN/GaN device had a current density 72.3 A/cm^2 , while the same epitaxial layer grown along the N-polar orientation had a comparable current density of 75 A/cm^2 . This indicates that GaN/GdN/GaN tunnel junctions have relatively weak dependence on crystal orientation and polarization in the reverse direction. However, in the forward bias, as shown in

Figure 2(b), the N-polar TJ shows higher current density than the Ga-polar TJ. This is because the polarization field in GdN is in the same direction as the depletion field in case of N-polar TJ. This effect is in fact quite similar to reduced turn-on voltage reported in previous work on N polar green LEDs²⁸.

To prove that inter-band tunneling does take place, we designed a n-GaN/GdN/p-GaN/n-GaN structure as shown in Fig 3 (a). This structure uses an n-GaN/GdN/p-GaN tunnel junction to contact the p-GaN layer of a GaN PN junction, thereby eliminating the need for a metal p-contact. As the PN junction is forward biased, the GaN/GdN tunnel junction is reverse biased. Electrons from the valence band of p-GaN tunnel into n-GaN, leaving a hole behind in the p-GaN layer. This is equivalent to tunnel injection of holes from an n-GaN contact into the p-type material, and so if the tunnel junction is ideal, we expect this structure to behave like a simple PN junction. The two important requirements for such a tunnel junction to be incorporated in a LED or solar cell would be that (1) the voltage drop across the tunnel junction during the device operation is negligible, with appreciable tunneling close to zero bias, and (2) the specific resistivity of the tunnel junction is minimal.

Growth and fabrication procedures described earlier in this Letter were used to obtain the device shown in Fig. 3(a). Atomic force microscope image of the sample surface shows typical step flow growth morphology with a low rms roughness of 0.6 nm. The structure with the GaN/GdN TJ contact layer was compared with a structure with a reference p⁺-n⁺ GaN TJ contact layer. As expected, the electrical characteristics of the device shown in Fig. 3 (c) were similar to that of a standard GaN PN junction. The forward turn on voltage of this device with the incorporation of a tunnel junction is the sum of the voltage drop across the forward biased p n junction and the voltage drop across the reverse biased tunnel junction. At a reference current density of 20 A/cm², the p contact-less PN junction with GaN/GdN TJ had a voltage drop of 3.15 V, compared to 4.5 V for the p⁺-n⁺ GaN TJ device . This indicates an additional voltage drop of 1.35 V across the p⁺-n⁺ GaN TJ, which is similar to past reports where a GaN based tunnel junction LEDs led to an extra voltage drop ranging from 0.6 V to 1.5 V^{29,30}. In contrast, the GaN/GdN TJ realized in this work behaves as an ideal tunnel junction with negligible voltage drop across it.

The resistance of the device with GaN/GdN TJ in forward bias was found, from a fit of the linear portion of the forward bias characteristics, to be $3.2 \times 10^{-3} \Omega\text{-cm}^2$. This includes the contact resistance, series resistance in the p-GaN and n-GaN regions, and the tunnel junction resistance. The top contact resistance was measured using transfer length method (TLM) method, and found to be $1.3 \times 10^{-5} \Omega\text{-cm}^2$. The p-GaN layer series resistance was calculated to be at least $4.4 \times 10^{-4} \Omega\text{-cm}^2$ assuming a hole mobility of $10 \text{ cm}^2/\text{Vs}$ and 1% ionization of Mg dopant. Neglecting the series resistance of n-type GaN and the bottom contact resistance (very large area contact), the specific tunnel junction resistivity can be extracted to be *less than* $2.7 \times 10^{-3} \Omega\text{-cm}^2$, which is the lowest reported series resistance for the III-nitride system. To benchmark these results against the literature, the lowest specific tunnel junction resistivities achieved in different material systems are compared in Figure 4^{3, 4, 31-38}. It is evident from the figure that tunnel resistivity increases exponentially with band gap, and that while low resistivity in wider band gap materials such as GaN is an inherent challenge, heterostructure engineering using GdN nanoparticles provides a new engineering route to overcome this limitation.

With the availability of a polarity-independent efficient tunnel junction, several promising applications and new directions for GaN electronics and optoelectronics can now be imagined. Several groups have indicated the advantages of N-polar P-up²⁸ or Ga-polar P-down¹⁵ LEDs. However, P-down LEDs have been unsuccessful due to the large p-type layer spreading resistance, and therefore need a tunnel junction to connect the p-layer to an n-type substrate. Heterostructure polarization engineering based approaches using InGaN are not effective since they work for N-polar oriented P-down PN tunnel junctions¹¹ and not for a Ga-polar oriented P-down PN junctions. The alternate approach (using GaN/AlN/GaN) could be used for the aforementioned cases, but does not provide low enough tunneling resistance to be useful^{9, 10}. The GdN approach overcomes these limitations by enabling both Ga-polar and N-polar oriented PN junctions. GdN nanoislands could also be embedded in wide band gap barriers, combining polarization and nanoparticle engineering for lower resistance. Previous work on GaN TJ LED^{29, 30, 38} showed an improved current spreading leading to enhanced light output. However the TJ LED devices had an additional voltage drop across the TJ. The efficient low resistance tunnel junction achieved

in this work can be incorporated to enhance the performance of top emitting LEDs. Another interesting application is the incorporation of low resistance tunnel junctions in vertical cavity emitters³⁹ where current spreading and resistance of p-type layers are major issues. The magnetic properties of GdN²³ and high tunneling current density could also enable new spintronic devices that benefit from the high spin lifetimes in GaN⁴⁰. The design of GaN bipolar devices such as PN diodes and BJTs has been limited by p-type contacts and resistance. Low resistance tunnel junctions can now be used to re-design these bipolar devices to achieve greater performance or functionality. Finally, since GdN-based junctions do not require polarization, they could also be used to improve performance for newly emerging non-polar and semi-polar GaN devices.

In summary, we demonstrated that epitaxial GdN nano islands can be used for efficient inter-band tunneling in GaN PN junctions on Ga- and N-polar tunnel junctions. Efficient tunnel injection of holes from n-type GaN top contact into p-type material was achieved, and the tunnel junction specific contact resistivity of GdN was determined to be lower than $2.7 \times 10^{-3} \Omega\text{-cm}^2$. This demonstration of efficient tunneling using GdN nanoislands, together with previously reported polarization-engineered tunnel junctions^{11,12} could lead to new designs for III-nitride electronic and optoelectronic devices with higher performance and functionality.

We acknowledge funding from ONR DATE MURI program (Program manager: Dr. Paul Maki).

References:

¹ L. Esaki, Phys. Rev. **109**, 603 (1958).

² R.R. King, D.C. Law, K.M. Edmondson, C.M. Fetzer, G.S. Kinsey, H. Yoon, R.A. Sherif, and N.H. Karam, Appl. Phys. Lett. **90**, 183516 (2007).

³ N. Jin, S.-Y. Chung, A.T. Rice, P.R. Berger, R. Yu, P.E. Thompson, and R. Lake, Appl. Phys. Lett. **83**, 3308 (2003).

- ⁴ K. Vizbaras, M. Törpe, S. Arafin, and M.-C. Amann, *Semi. Sci. and Tech.* **26**, 075021 (2011).
- ⁵ M.J. Grundmann and U.K. Mishra, *Phys. Status Solidi C* **4**, 2830 (2007).
- ⁶ C.J. Neufeld, N.G. Toledo, S.C. Cruz, M. Iza, S.P. DenBaars, and U.K. Mishra, *Appl. Phys. Lett.* **93**, 143502 (2008).
- ⁷ F. Bernardini, V. Fiorentini, and D. Vanderbilt, *Phys. Rev. B* **56**, R10024 (1997).
- ⁸ C. Wetzel, T. Takeuchi, H. Amano, and I. Akasaki, *J. of Appl. Phys.* **85**, 3786 (1999).
- ⁹ M.J. Grundmann, J.S. Speck, and U.K. Mishra, in *Device Research Conference Digest, 2005. DRC '05. 63rd* (IEEE, 2005), pp. 23–24.
- ¹⁰ J. Simon, Z. Zhang, K. Goodman, H. Xing, T. Kosel, P. Fay, and D. Jena, *Phys. Rev. Lett.* **103**, 026801 (2009).
- ¹¹ S. Krishnamoorthy, D.N. Nath, F. Akyol, P.S. Park, M. Esposito, and S. Rajan, *Appl. Phys. Lett.* **97**, 203502 (2010).
- ¹² S. Krishnamoorthy, P.S. Park, and S. Rajan, *Appl. Phys. Lett.* **99**, 233504 (2011).
- ¹³ J.-H. Lee and J.-H. Lee, *Elec. Dev.Lett., IEEE* **31**, 455 (2010).
- ¹⁴ S. Krishnamoorthy, F. Akyol, J. Yang, P. S. Park, R. Myers, S. Rajan, in *Device Research Conference Digest, 2012. DRC '12, 70th* (IEEE, 2012).
- ¹⁵ M.L. Reed, E.D. Readinger, H. Shen, M. Wraback, A. Syrkin, A. Usikov, O.V. Kovalenkov, and V.A. Dmitriev, *Appl. Phys. Lett.* **93**, 133505 (2008).
- ¹⁶ F. Akyol, D.N. Nath, E. Gür, P.S. Park, and S. Rajan, *Jpn. J. Appl. Phys.* **50**, 052101 (2011).
- ¹⁷ S. Ahmed, M.R. Melloch, E.S. Harmon, D.T. McInturff, and J.M. Woodall, *Appl. Phys. Lett.* **71**, 3667 (1997).
- ¹⁸ C. Kadow, S.B. Fleischer, J.P. Ibbetson, J.E. Bowers, A.C. Gossard, J.W. Dong, and C.J. Palmstrøm, *Appl. Phys. Lett.* **75**, 3548 (1999).

- ¹⁹ P. Pohl, F.H. Renner, M. Eckardt, A. Schwanhäußer, A. Friedrich, Ö. Yüksesdag, S. Malzer, G.H. Döhler, P. Kiesel, D. Driscoll, M. Hanson, and A.C. Gossard, *Appl. Phys. Lett.* **83**, 4035 (2003).
- ²⁰ F.L. Bloom, A.C. Young, R.C. Myers, E.R. Brown, A.C. Gossard, and E.G. Gwinn, *J. Vac. Sci. Technol. B* **24**, 1639 (2006)
- ²¹ J.M.O. Zide, A. Kleiman-Shwarsctein, N.C. Strandwitz, J.D. Zimmerman, T. Steenblock-Smith, A.C. Gossard, A. Forman, A. Ivanovskaya, and G.D. Stucky, *Appl. Phys. Lett.* **88**, 162103 (2006).
- ²² S.A. Wolf, D.D. Awschalom, R.A. Buhrman, J.M. Daughton, S. Von Molnár, M.L. Roukes, A.Y. Chtchelkanova, and D.M. Treger, *Science* **294**, 1488 (2001).
- ²³ S. Dhar, O. Brandt, M. Ramsteiner, V.F. Sapega, and K.H. Ploog, *Phys. Rev. Lett.* **94**, 037205 (2005).
- ²⁴ W.R.L. Lambrecht, *Phys. Rev. B* **62**, 13538 (2000).
- ²⁵ M.A. Scarpulla, C.S. Gallinat, S. Mack, J.S. Speck, and A.C. Gossard, *J. of Crys. Growth* **311**, 1239 (2009).
- ²⁶ T.F. Kent, J. Yang, L. Yang, M.J. Mills, and R.C. Myers, *Appl. Phys. Lett.* **100**, 152111 (2012).
- ²⁷ Saint Gobain Crystals, Vallarius, France.
- ²⁸ F. Akyol, D.N. Nath, S. Krishnamoorthy, P.S. Park, and S. Rajan, *Appl. Phys. Lett.* **100**, 111118 (2012).
- ²⁹ S. R. Jeon, Y. H. Song, H. J. Jang, G. M. Yang, S. W. Hwang, and S. J. Son, *Appl. Phys. Lett.* **78**, 3265 (2001).

- ³⁰ T. Takeuchi, G. Hasnain, S. Corzine, M. Hueschen, Jr. Schneider, C. Kocot, M. Blomqvist, Y. Chang, D. Lefforge, M. R. Krames, L. W. Cook, and S. A. Stockman, *Jpn. J. Appl. Phys.* **40**, L861 (2001).
- ³¹ M.P. Lumb, M.K. Yakes, M. González, I. Vurgaftman, C.G. Bailey, R. Hoheisel, and R.J. Walters, *Appl. Phys. Lett.* **100**, 213907 (2012).
- ³² H.P. Nair, A.M. Crook, and S.R. Bank, *Appl. Phys. Lett.* **96**, 222104 (2010).
- ³³ S. Preu, S. Malzer, G.H. Döhler, H. Lu, A.C. Gossard, and L.J. Wang, *Semi. Sci. and Tech.* **25**, 115004 (2010).
- ³⁴ N. Suzuki, T. Anan, H. Hatakeyama, and M. Tsuji, *Appl. Phys. Lett.* **88**, 231103 (2006).
- ³⁵ P.R. Sharps, N.Y. Li, J.S. Hills, H.Q. Hou, P.C. Chang, and A. Baca, in *Conference Record of the Twenty-Eighth IEEE Photovoltaic Specialists Conference, 2000* (IEEE, 2000), pp. 1185–1188.
- ³⁶ M. J. Grundmann, Ph. D. Dissertation, University of California, Santa Barbara (2007).
- ³⁷ J.K. Sheu, J.M. Tsai, S.C. Shei, W.C. Lai, T.C. Wen, C.H. Kou, Y.K. Su, S.J. Chang, and G.C. Chi, *Elec. Dev. Lett., IEEE* **22**, 460 (2001).
- ³⁸ S. Jin An, *Appl. Phys. Lett.* **100**, 223115 (2012).
- ³⁹ M. Diagne, Y. He, H. Zhou, E. Makarona, A.V. Nurmikko, J. Han, K.E. Waldrip, J.J. Figiel, T. Takeuchi, and M. Krames, *Appl. Phys. Lett.* **79**, 3720 (2001).
- ⁴⁰ B. Beschoten, E. Johnston-Halperin, D.K. Young, M. Poggio, J.E. Grimaldi, S. Keller, S.P. DenBaars, U.K. Mishra, E.L. Hu, and D.D. Awschalom, *Phys. Rev. B* **63**, 121202 (2001).

Figure captions:

Figure 1: (Color online) Equilibrium charge profile and band diagram of (a) Ga-polar, and (b) N-polar oriented p-GaN/ GdN/ n-GaN TJ. Polarization and depletion fields are aligned for the N-polar orientation case. Effect of increased doping in the case of (c) Ga-polar, and (b) N-polar p-GaN/ GdN/ n- GaN TJ.

Figure 2: (Color online) (a) Epitaxial stack of GaN/GdN/GaN inter-band tunnel junction (b) I-V characteristics of Ga-polar and N-polar GaN/GdN/GaN TJ . Reverse characteristics of the Ga-polar and N-polar TJ shows similar current density indicating a weak polarization dependence on tunneling resistance.

Figure 3: (Color online) (a) Epitaxial stack of the p-contactless PN junction where a GaN/GdN TJ connects the p-region with the n-region. The energy band diagram shows tunnel injection of holes into p-type material from the n-type contact when the PN junction is forward biased. (b) Atomic force microscope image showing smooth surface morphology (rms roughness = 0.6 nm) (c) J- V characteristics of the p-contactless PN junction with and without GaN/GdN TJ. The sample with GaN/GdN TJ has negligible voltage drop across it, while the reference sample has a significant resistive drop.

Figure 4: (Color online) Plot of specific tunnel junction resistivity achieved in different material systems as a function of band gap. The work presented here represents the lowest reported specific tunneling resistance in GaN, marked as a star in the plot.

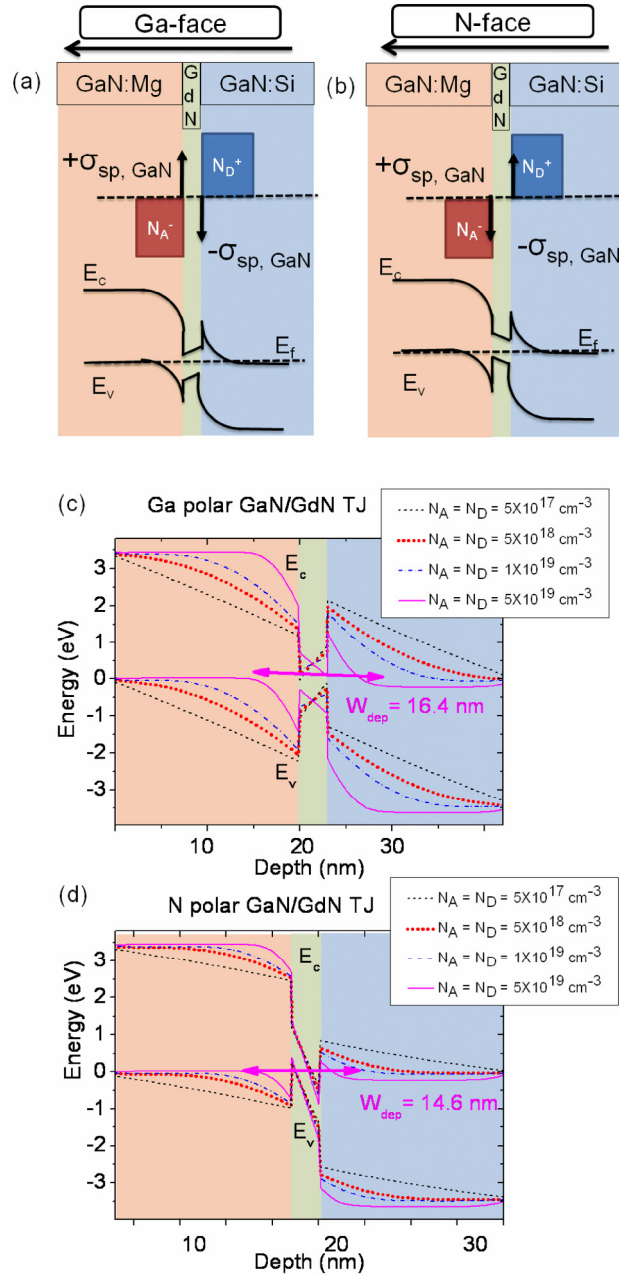


Fig 1

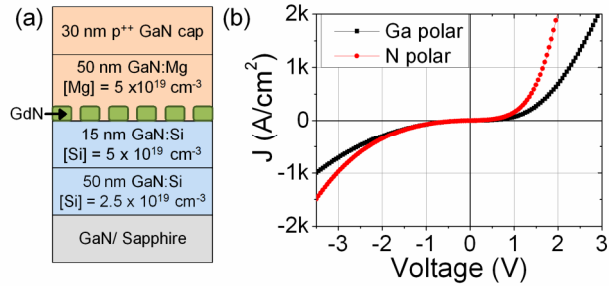


Fig 2

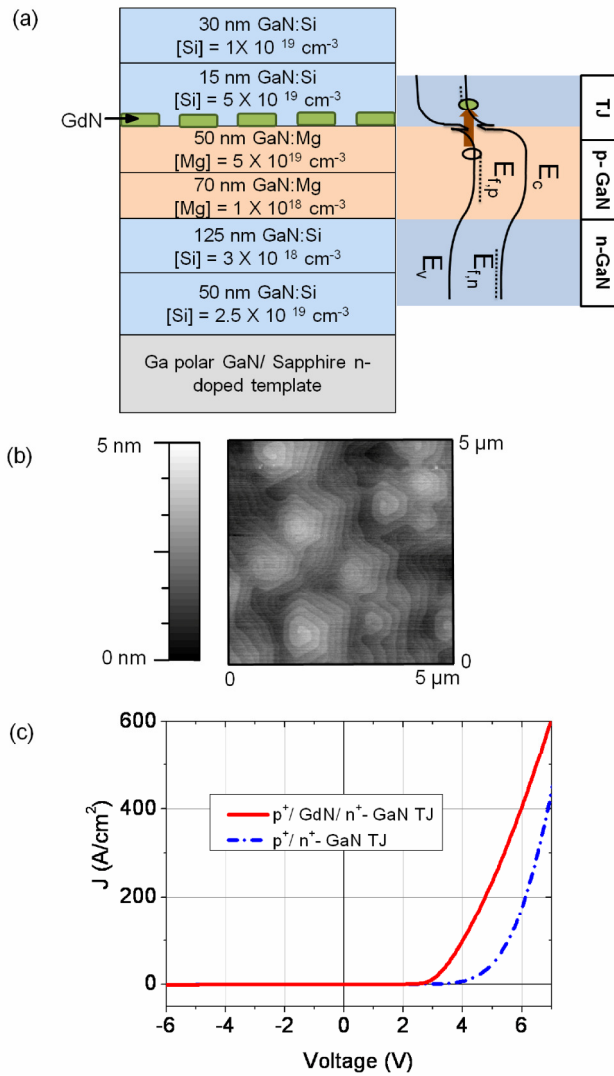


Fig. 3

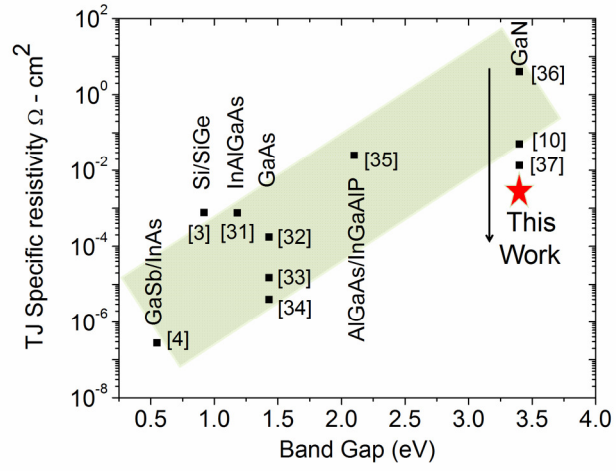


Fig 4.